# Effect of Quantum Confinement on Thermoelectric Properties of 2D and 1D Semiconductor Thin Films

**A. Bulusu and D. G. Walker[1]**

**Interdisciplinary Program in Material Science**
**Vanderbilt University**
**Nashville, TN 37235**

With device dimensions shrinking to nanoscales, quantum effects such as confinement and tunneling become significant in electron transport. In addition, scattering effects such as electron-phonon scattering, electron-impurity scattering also affect carrier transport through small-scale devices. Currently most of the commonly used transport models are particle based with quantum corrections incorporated to include quantum effects while models based on the solution to the Schrödinger wave equation can be computationally intensive. In this regard, the NEGF formalism has been found to be very efficient in coupling quantum and scattering effects. In this paper the NEGF model is used to assess the effect of temperature on device characteristics of 1D and 2D thin film superlattices whose applications include thermoelectric cooling of electronic and optoelectronic systems. The effect of quantum confinement on the electrical transport and its impact on the thermoelectric figure of merit is studied in the two cases. Results show a competing effect between the electrical and thermal conductivity on the overall figure of merit in the two dimensionally confined thin films.

## INTRODUCTION

The two fundamental aspects that differentiate nanoscale device modeling from bulk modeling are scattering effects and quantum effects. Scattering in nanostructures can significantly affect carrier as well as thermal transport in devices. Inelastic electron-phonon scattering can cause electrons to lose or gain energy with the lattice while other scattering effects such as carrier-carrier, carrier-defect, and carrier-boundary scattering can lead to energy redistribution in devices where transport is near ballistic. Quantum effects manifest themselves in the form of electron tunneling as well as carrier confinement. These effects usually dominate when the device length scales are of the order of the de Broglie wavelength associated with the device. Quantum confinement can lead to reduced density of states available for the carrier while electron tunneling can have a detrimental impact in the form of leakage currents in very small sized transistors [1]. However, quantum effects can be very useful as a high performance alternative to very-large-scale integration (VLSI) [2] in the form of resonant tunneling diodes.

In general carrier transport models can be classified into two types. The first type is the classical particle models that are based on finding the solution to the Boltzmann transport equation (BTE). The second type involves a direct solution to the Schrödinger wave equation. Quantum effects in the BTE based models are included by incorporating a quantum correction to the transport model. Common methods of incorporating quantum effects are the density gradient formalism and the effective potential method [3]. The density gradient formalism is derived from the equation of motion for the one particle Wigner function where quantum corrections are introduced by expressing the mean potential energy as a power series in $h$. The transport equation for the Wigner distribution function can now be written in the form of a modified Boltzmann Transport Equation. The effective potential method involves a localized wavepacket representation of the carriers associated with an effective potential obtained by summing the inhomogeneous potential introduced in the Hamiltonian, over all the carriers. The generation of the effective potential determines the onset of quantization in the system. The quantum correction methods have been found to give an excellent match with the Poisson-Schrodinger solver for the case of carrier confinement and tunneling. More recently, attempts have been made to combine quantum corrections with the Monte Carlo technique [4] which is a numerical solution to the BTE. The results have been found to match well with the Schrodinger solution in the case of carrier confinement while a reasonably close match was observed for the case of tunneling. However, extension of this model to 2 and 3 dimensions remains, computationally tedious and difficult.

Quantum transport models that involve the solution to the Schrödinger wave equation can be used to study current flow over small scales where the transport can be either ballistic or can involve some type of scattering. The main models used to model ballistic transport are Quantum Transmitting Boundary Model (QTBM) [5] and the Quantum Device Analysis by Mode Evaluation (QDAME) [6]. QTBM involves formulating the boundary conditions for a given problem by calculating the transmission and reflection coefficients for a known boundary potential. These boundary conditions are then used in a numerical solution based on the finite element method to obtain the wave function over the entire problem domain. While this method is suitable for solving the Schrödinger equation for various boundary potentials, inclusion of dissipation due to scattering becomes very difficult to solve using this method. QDAME involves discretely sampling a device's density of states using standing wave boundary conditions. The standing

[1] Corresponding author; greg.walker@vanderbilt.edu

waves are decomposed into traveling waves and injected from the contacts from which their occupancies are assigned.

Shrinking device dimensions present an increasing need for a simple quantum transport model that can effectively couple quantum and scattering effects. The non-equilibrium Green's function formalism provides a framework for natural coupling of quantum and scattering effects. Open boundary conditions allow the source and drain contacts to be coupled to the device through simple self-energy terms that helps eliminate working with huge matrices that are of the size of the source and drain reservoir systems and instead work with matrices that are the size of the device Hamiltonian. In addition, the NEGF formalism allows for the rigorous incorporation of both elastic and inelastic scattering effects using the concept of Buttiker probes where scattering is treated as another contact, allowing it to be coupled to the device using self-energy terms. We present a brief synopsis of the formalism in the next section while a more thorough and detailed development can be found in [7] and [8].

A significant amount of research has gone into enhancing the thermoelectric figure of merit ZT = $S^2\sigma/\kappa$ where S is the Seebeck coefficient, $\sigma$ is the electrical conductivity and $\kappa$ is the thermal conductivity. In this regard, quantum well heterostructures have gained attention as thermoelectric materials due to their reduced thermal conductivities [9, 10, 11]. Phonon interference effects caused by phonon-interface scattering give rise to bandgaps at the interface of the thin films in a superlattice, affecting phonon transport through these structures. In addition, electron-phonon scattering in the superlattice affects electron transport through the device, which eventually affects the thermoelectric figure of merit. Chen [12, 13] studied the phonon transport in SiGe superlattices using the BTE for phonons. Phonon interface scattering was included through a combination of diffuse and specular scattering. While the emphasis of present research is on heat transfer through phonon transport in superlattices, the effect of quantum confinement on the electrical conductivity is also important in the performance of thermolectrics. Using the structure in [12, 13] as a model system we use the NEGF formalism to study the effect of temperature and quantum confinement on the electrical properties of 2D thin film thermoelectric layer. The effect of carrier confinement on the electrical conductivity and the thermoelectric figure of merit are studied by reducing one of the macroscopic dimensions of the 2D film leading to confinement of electrons in two dimensions. The 2D and 1D films are modeled to be ballistic in nature. Future work is focused towards studying the device characteristics under the influence of temperature and electron-phonon scattering in Si and SiGe nanowire superlattices while incorporating the effects of phonon interface scattering.

## THE NEGF FORMALISM

In general an isolated device and its energy levels are described using a Hamiltonian matrix where *H* is the Hamiltonian; *U* is the Hartree potential and $\alpha$ the energy eigen state of the electron.

$$(H+U)\psi_\alpha(\vec{r}) = \varepsilon_\alpha \psi_\alpha(\vec{r}). \qquad (1)$$

The electron density matrix in real space is given by

$$\left[\rho(E,\vec{r},\vec{r}'\right] = \int_{-\infty}^{+\infty} dE\, f\left(E+\varepsilon_k-\mu\right)\delta([EI-H]). \qquad (2)$$

where *f* is the Fermi function. For a two dimensional film the Fermi function is given by considering the electrons to have free flow along the x and y directions and experience confinement along the z direction.

$$f_{2D} = N_0 \ln[1+\exp\left(\frac{-E}{k_BT}\right) \text{ where } N_0 = \frac{m_c k_B T}{2\pi\hbar^2}. \qquad (3)$$

The Fermi function for a 1D film is calculated in a similar manner by considering the electron to have free flow only in the x direction. $f_{1D}$ is given by

$$f_{1D} = \frac{N}{4\pi} f_{-1/2}(x) \text{ where } N = \sqrt{\frac{2m_c k_B T}{\hbar^2}}. \qquad (4)$$

The value of x is given by $x = \dfrac{\hbar^2 k_x^2}{2m_c k_B T}$.

*δ(EI-H)* is the local density of states. Using the standard expansion for the delta function we get

$$\delta(EI-H) = \frac{i}{2\pi}\left(\left[\left(E+i0^+\right)I-H\right]^{-1} - \left[\left(E-i0^+\right)I-H\right]^{-1}\right). \qquad (5)$$

From the above equation, the delta function can also be written as

$$\delta(EI-H) = \frac{i}{2\pi}\left[G(E)-G^+(E)\right];$$

$$G(E) = \left[\left(E-i0^+\right)I-H\right]^{-1}. \qquad (6)$$

*G(E)* is the retarded Green's function while $G^+(E)$ is its conjugate complex transpose. The Green's function can be interpreted as the impulse response of the Schrödinger equation that will give us the $n^{th}$ component of the wave function if the system is given an impulse excitation at the $m^{th}$ component. The density of states in real space is given by the spectral function, which can be interpreted as the available density of states that are filled up according to the Fermi function so as to obtain the electron density. The diagonal elements of the spectral function represent the local electron density of states,

$$A(\vec{r},\vec{r}',E) = 2\pi\delta(EI-H) = i\left[G(E)-G^+(E)\right]. \qquad (7)$$

Thus the electron density matrix for an isolated device can also be written in the form

$$\left[\rho_k\right] = \int_{-\infty}^{+\infty} \frac{dE}{2\pi} f_0\left(E+\varepsilon_k-\mu\right) A(E)]. \qquad (8)$$

Now consider the case of a simple nanotransistor consisting of source and drain contacts. Let $\mu_1$ and $\mu_2$ be the chemical potentials of the source and the drain. The distribution of electrons in the source and drain is said to follow the Fermi distribution where $f_1$ and $f_2$ are the Fermi functions of the source and drain. The difference in the Fermi levels of the source and drain causes electrons to flow from the source to the drain through the channel. The average number of electrons $N$ at steady state will lie between $f_1$ and $f_2$ i.e. $f_1 < N < f_2$. When no scattering is incorporated the channel can be considered to be ballistic in nature and is expected to have zero resistance to current flow. However, experimental measurements [14] have shown that the maximum measured conductance of a one-energy level channel approaches a limiting value $G_0 = 2q^2/\hbar = 51.6(K\Omega)^{-1}$. The reason for this limit to conductance arises from the fact that current in the contacts is carried by infinite transverse modes while the number of available modes in the channel is limited. This means that the density of states in the contacts is spread over a large energy range while the channel density of states lies specifically between $\mu_1$ and $\mu_2$. Upon coupling the contact and the channel, some of the density of states from the contact spread into the channel while the channel loses some of its density of states to the contact. As a result, the coupling causes the density of states in the channel to spread out over a wider range of energy levels resulting in a reduction in the number of states lying between $\mu_1$ and $\mu_2$. Consequently, the overall effect of the coupling is to broaden the range of energy levels of the channel leading to a reduction in the number of states in the range $\mu_1$ to $\mu_2$ that are available for electron flow through the channel. In the NEGF formalism the coupling of the device to the source and drain contacts is described using self-energy matrices $\Sigma_1$ and $\Sigma_2$. The self-energy term can be viewed as a modification to the Hamiltonian to incorporate the boundary conditions. Accordingly, equation 1 and 4 can be rewritten as

$$\left(H + U + \Sigma_1 + \Sigma_2\right)\psi_\alpha(\vec{r}) = \varepsilon_\alpha \psi_\alpha(\vec{r}) \qquad (9)$$

$$G(E) = \left[\left(E - i0^+\right)I - H - \Sigma_1 - \Sigma_2\right]^{-1}. \qquad (10)$$

The rate at which an electron is extracted from the reservoir is dependent on $i0^+$, an infinitesimal term added to the energy of the device eigenstate that will ensure that the system behaves irreversibly as long as it exceeds the spacing between the energy levels in the reservoirs. Appropriate values of $i0^+$ will ensure that an electron always travels from the reservoir into the channel and not vice-versa. The broadening of the energy levels introduced by connecting the device to the source and drain contacts is incorporated through the Gamma functions $\Gamma_1$ and $\Gamma_2$ given by

$$\Gamma_1 = i(\Sigma_1 - \Sigma_1^+) \qquad \Gamma_2 = i(\Sigma_2 - \Sigma_2^+) \qquad (11)$$

The self-energy terms affect the Hamiltonian in two ways. The real part of the self-energy term shifts the device eigenstates or energy level while the imaginary part of $\Sigma$ causes the density of states to broaden while giving the eigenstates a finite lifetime. The effect of the self-energy terms is shown in equation

$$H + \Sigma(E) = \left[H + \Sigma_H(E)\right] - \frac{i\Gamma(E)}{2} \qquad \text{where}$$

$$\Sigma_H = \frac{1}{2}\left[\Sigma(E) + \Sigma^+(E)\right]. \qquad (12)$$

The lifetime of the eigenstate can be related to the self-energy through the equation

$$\frac{1}{\tau} = \frac{\gamma}{\hbar} = -\frac{2\,\mathrm{Im}\,\Sigma}{\hbar}. \qquad (13)$$

Following the above argument, the Green's function for a given eigenstate can also be written as

$$G(E) = \frac{1}{(E - \varepsilon') + i\gamma/2}. \qquad (14)$$

where $\varepsilon' = \varepsilon + \sigma$. $\varepsilon$ corresponds to the energy of the eigenstate while $\sigma$ corresponds to the energy increment due to coupling of the self-energy function. The corresponding density of states due to the broadening, take the form

$$\frac{A(E)}{2\pi} = D(E) = i\left(G(E) - G^+(E)\right). \qquad (15)$$

The electron density for the open system is given by

$$[\rho] = \int_{-\infty}^{+\infty}\left(\frac{dE}{2\pi}\right)\left[G^n(E)\right]. \qquad (16)$$

$G^n(E)$ represents the electron density per unit energy and is given by

$$G^n = G\Sigma^{in}G^+ \quad \text{where} \quad [\Sigma^{in}] = [\Gamma_1]f_1 + [\Gamma_2]f_2. \qquad (17)$$

The source, drain and scattering self-energy terms are used to obtain the final Green's function from which the net channel current is calculated as a difference in the inflow and outflow currents using equations 18, 19 and 20. The entire calculation is carried out self-consistently with Poisson's equation to account for the change in channel potential with the change in electron density.

$$\text{Inflow} = \frac{1}{\hbar}\int\frac{dE}{2\pi} f_0(E - \mu)\,Trace[\Gamma A] \qquad (18)$$

$$\text{Outflow} = \frac{1}{\hbar}\int\frac{dE}{2\pi} Trace\left[\Gamma G^n\right] \qquad (19)$$

$$I_i = \frac{-q}{\hbar}\int_{-\infty}^{+\infty} Trace[\Gamma_i A]f_i - Trace\left[\Gamma_i G^n\right] \qquad (20)$$

## RESULTS

### Thermoelectric effects in silicon 2D and 1D thin films

Two kinds of thin films were studied in this paper as shown in figure 1. The first was a 2D Silicon thin film with infinite

dimension in x and y while the z direction had a thickness of 30nm. The second film is a 1D thin film with infinite dimension in the y direction while the x and z directions have thickness of 6nm. The thermopower for silicon thin film was studied for various temperature ranges of the source and drain contacts while varying the doping in silicon. The source temperature was maintained constant at 300K while the drain contact was maintained a higher temperature relative to the source. The applied bias ranged from 0 to 0.25V.

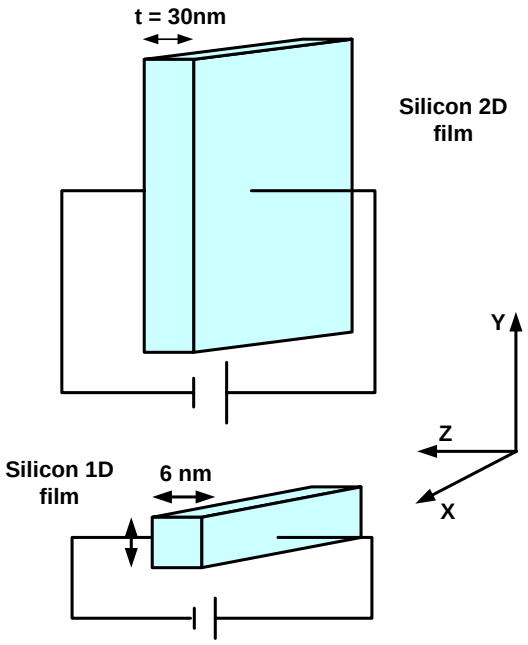


**Figure 1. Schematic diagram of 2D and 1D Silicon thin films with 1D and 2D confinement.**

Figure 2 shows the current-voltage characteristics for a ballistic silicon 2D thin film doped to electron concentration of $5x10^{18}cm^{-3}$. The source-drain temperature difference ranges from 0K to a maximum of 50K. Initially for low bias conditions, the number of high energy electrons generated in the drain contact is higher than the number of electrons arriving at the drain through the channel leading to negative current values. As the bias in increased gradually, more electrons from the source are drawn towards the drain due to the applied bias leading to higher inflow at the drain leading to positive current values.

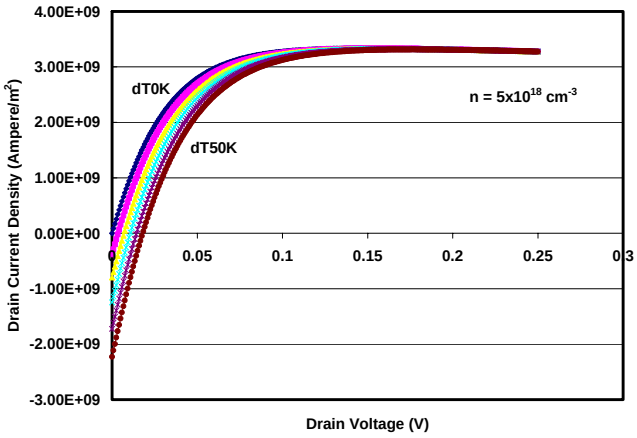


**Figure 2. Current-voltage characteristics of a ballistic silicon thin film with doping level of $5x10^{18}cm^{-3}$. Channel temperature variation ranges from 0K to 50K.**

Figure 3 shows the averaged predicted and measured Seebeck coefficient values for 2D and 1D silicon films for various doping levels in all temperature ranges considered. The predicted values of S differ from the measured values approximately by a factor of 2 indicating good agreement [15]. In addition, the calculated Seebeck coefficients for the 2D and 1D silicon films are very close to each other proving the fact that the Seebeck coefficient is a material property and is independent of the effects of quantum confinement.

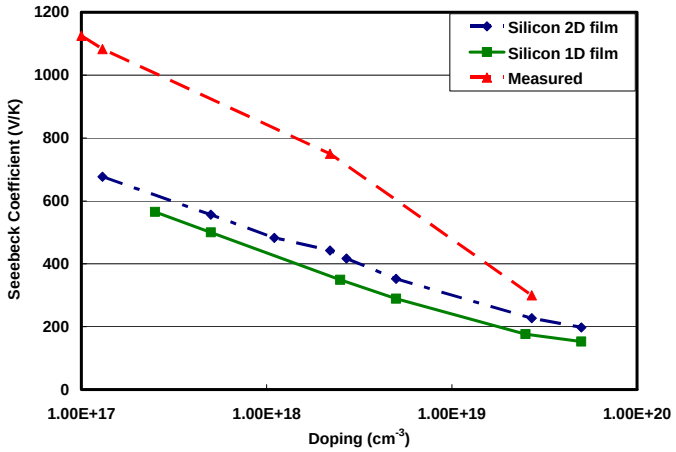


**Figure 3. Predicted vs. measured [15] values of Seebeck coefficient for silicon at 300K as a function of doping levels.**

The effect of carrier confinement two dimensions has contrasting influences on the thermoelectric figure of merit ZT due to thermal and electrical conductivity. Confining phonons in two dimensions leads to increased phonon boundary scattering resulting in a decrease in thermal conductivity than the 1D value. However, the decrease in available electron density of states with 2D confinement leads to a drastic reduction in the electrical conductivity as seen in figure 4.

6 nm

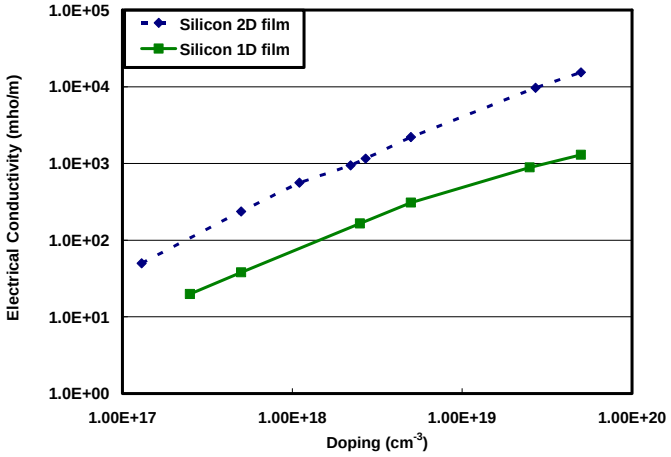


**Figure 4. Comparison of electrical conductivity values for a Silicon 2D film and Silicon 1D film.**

The change in ZT with doping for 2D and 1D silicon thin film is shown in figure 5. The competing effect of the decreasing thermal conductivity with the decrease in electrical conductivity for the two cases is very obvious especially at higher doping levels. At high doping levels while the number of electrons available for transport is high, the reduced density of states in the 1D film leads to 12 times as much resistance to the flow of electrons compared to the 2D film where more density of states are available to transport the available electrons. Since the Seebeck coefficient does not change significantly for both cases, the increase in ZT by reduced thermal conductivity of the 1D film can be offset by the reduced electrical conductivity. It should be noted that in addition to the decrease in the film thickness from infinity to 6nm in the y-dimension, the difference in the thickness of the two films from 30nm to 6nm in the z direction may also lead to additional confinement effects in the z direction causing the overall reduction in electrical conductivity. Current work is focused towards modeling and comparing films with identical thickness in the z-direction.

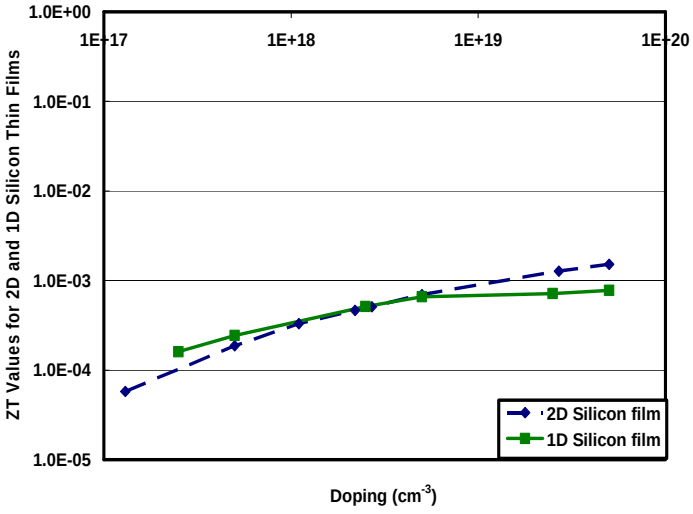


**Figure 5. Change in ZT values with 1D and 2D carrier confinement. $k_{Si}$ (2D) = 131W/m-K [16], $k_{si}$ (1D) = 13 W/m-K [17].**

**Thermoelectric effects in SiGe 2D and 1D thin films**

The thermoelectric properties of SiGe 2D and 1D superlattice films were studied in a similar manner by maintaining the drain at higher temperature than the source. For the 2D film each of the semiconductor thin films was 15nm thick leading to a combined thickness of 30nm. The source temperature was maintained at 300K while the drain temperature values were varied from 310K to 350K. Silicon and Germanium were both degenerately doped to values ranging from $2.5x10^{17}$ $cm^{-3}$ to $8.5x10^{19}cm^{-3}$. The predicted value of the Seebeck coefficient in the case of the 2D film for the $8.5x10^{19}cm^{-3}$ doping level was found to be 160μV/K, which is a good match to the experimentally measured value of 312μV/K in [16].

The 1D superlattice films were each modeled as having a square cross-section of 3nm x 3nm leading to an over all superlattice cross-sectional area of 6nm x 6nm. The superlattice film was considered to be infinitely long in the x-direction. While the source was maintained at a temperature of 300K, the temperature of the drain had to be increased to a minimum value of 430K to notice any significant thermoelectric effects. The reason for this behavior was attributed to the fact that a 6nm thick device behaves as a ballistic device having almost no resistance to electron flow. In order for the electrons to gain sufficient thermal energy so as to travel in a direction opposite to the applied field they have to be excited to very high energy levels. These energy levels were achieved only by increasing the drain temperature to at least 430K. Figure 6 shows the Seebeck coefficients of the 2D and 1D SiGe films. The difference in the calculated values of S for both cases varied approximately by 50μV/K proving that S is a material property.

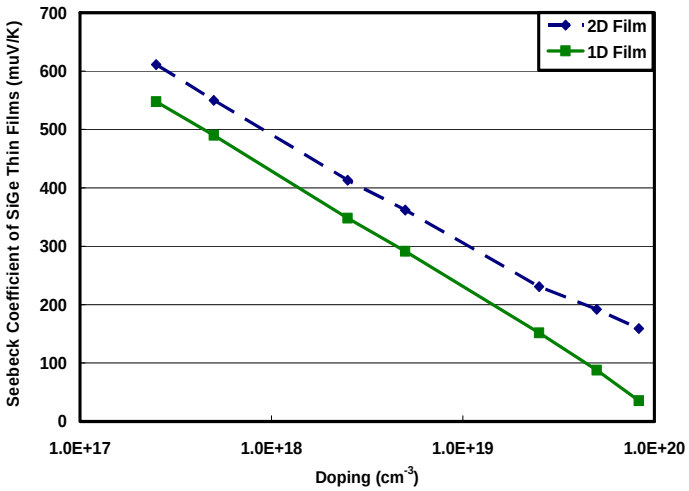


**Figure 6. Seebeck coefficient for SiGe 2D and 1D superlattice films for various doping levels.**

As in the case of silicon films the reduced density of states due to confinement in 2D caused the electrical conductivity for the SiGe films to decrease significantly when the y-dimension of the 2D superlattice thin film was reduced from infinity to 6nm changing it into a 1D superlattice film as seen in figure 7.

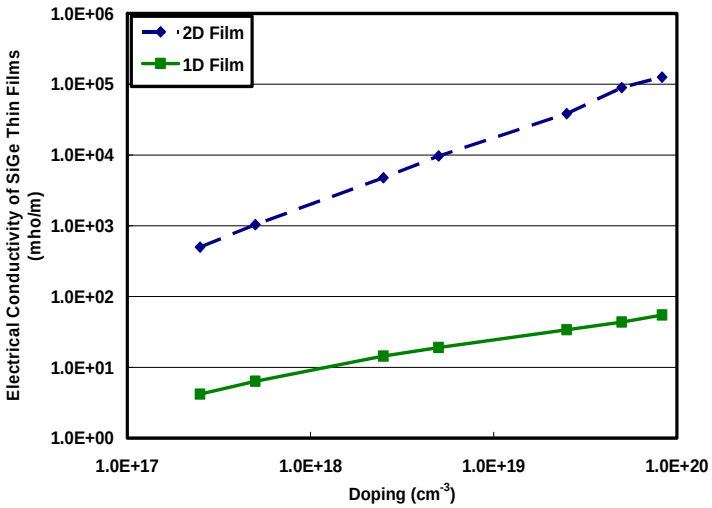


**Figure 7. Comparison of electrical conductivity of SiGe 2D and 1D superlattice thin films for various doping levels.**

The effect of the change in electrical conductivity and thermal conductivity with increasing confinement is evident from the change in ZT values.

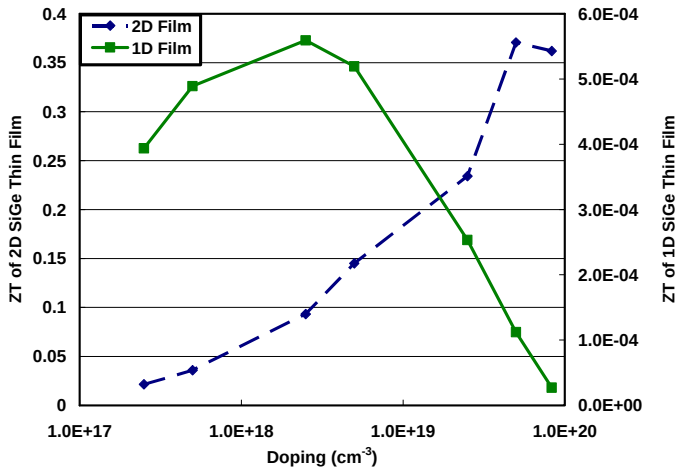


**Figure 8. Thermoelectric figure of merit for the 2D and 1D SiGe superlattice films, $k_{SiGe}$ (2D) = 2.92W/m-K [16], $k_{SiGe}$ (1D) = 1.45 W/m-K.**

The value of the thermal conductivity in the case of Si/SiGe superlattice nanowires was found to reduce by approximately a factor of 2 due to alloy scattering and increased boundary scattering [18, 19]. Using this ratio as a reference, the value of thermal conductivity for SiGe 1D thin film was taken to be half of that of the 2D film. While the Seebeck coefficient remained the same for both cases, the decrease in thermal conductivity due to increased confinement effects is more than compensated by the decrease in electrical conductivity due to a sharp drop in available density of states. As a result, the overall ZT value dropped by 2 to 4 orders of magnitude in the case of the 1D SiGe superlattice film compared to the 2D film.

## CONCLUSIONS

The non-equilibrium Green's function formalism was used to study the effects of quantum confinement on the thermoelectric behavior of electrons in 2D and 1D silicon and SiGe superlattice films. The increase in confinement from 2D to 1D film manifests itself in the form of reduced electron density of states leading to a sharp decline in the electrical conductivity of the films. While the increased confinement is believed to decrease the thermal conductivity due to boundary scattering, the simultaneous drop in electrical conductivity causes the overall thermoelectric figure of merit to not change significantly in the case of silicon films. In the case of the SiGe superlattice films, the decrease in electrical conductivity is steeper causing the figure of merit to reduce from 2 to 4 orders of magnitude for 2D confinement.

## ACKNOWLEDGMENTS

We are grateful to Prof. Supriyo Datta, Dept. of Electrical and Computer Engineering, Purdue University, for providing us with the manuscript of his book on which much of this work is based. This research was funded through the Vanderbilt Discover Grant

## REFERENCES

[1] Rahman, A., Ghosh, A and Lundstrom, M., 2003, "Assessment of Ge n-MOSFETs by Quantum Simulation," *Technical Digest of International Electronic Devices Meeting*, pp. 471-473.

[2] Mazumder, P., Kulkarni, S., Bhattacharya, M., Sun, J. P. and Haddad, G.I., 1998, "Digital circuit applications of resonant tunneling devices," *Proceedings of the IEEE*, **86**, **4**, pp. 664-686.

[3] Asenov, A., Watling, J. R., Brown, A. R. and Ferry, D. K., 2002, "The Use of Quantum Potentials for Confinement and Tunneling in Semiconductor Devices," *Journal of Computational Electronics*, **1**, pp.503–513.

[4] Tang, T. W. and Wu, B., 2004, "Quantum Correction for the Monte Carlo Simulation via the Effective Conduction-band Edge Equation," *Semiconductor Science and Technology*, **19**, pp. 54-60.

[5] Lent, C., S. and Kirkner, D., J., 1990, "The Quantum Transmitting Boundary Method," Journal of Applied Physics, **67**, **10**, pp. 6353-6359.

[6] Laux, S., E., Kumar, A. and Fischetti, M., V., 2002, "Ballistic FET Modeling Using QDAME: Quantum Device Analysis by Modal Evaluation," *IEEE Transactions on Nanotechnology*, **1**, **4**, pp. 255-259.

[7] Datta, S., 2000, "Nanoscale Device Simulation: The Green's Function Formalism," Superlattices and Microstructures, **28**, pp. 253-278.

[8] Datta, S., 2005, "*Quantum Transport: Atom to Transistor*," Cambridge University Press, New York.

[9] Hicks, L.D. and Dresselhaus, M. S., 1993, "Effect of Quantum Well Structures on the Thermoelectric Figure of Merit," *Physical Review B*, **47**, **12**, pp. 727-731.

[10] Whitlow, L. W. and Hirano, T., 1995, "Superlattice Applications to Thermoelectricity," *Journal of Applied Physics*, **78**, **9**, pp.5460-5466.

[11] Hicks, L. D., Harman, T. C. and Dresselhaus, M. S., 1993, "Use of Quantum-well Superlattices to Obtain a High Figure of Merit from Non-conventional Thermoelectric Materials," *Applied Physics Letters*, **63**, **23**, pp.3230-3232.
[12] Chen, G., 1998, "Thermal Conductivity and Ballistic-Phonon Transport in the Cross-Plane Direction of Superlattice," *Physical Review B*, **57**, **23**, pp. 14958-14973.
[13] Chen, G., 1999, "Phonon Wave Heat Conduction in Thin Films and Superlattices," *Journal of Heat Transfer*, **121**, pp. 945-953.
[14] Szafer, A. and Stone, A. D., 1989, "Theory of Quantum Conduction through a Constriction," *Physical Review Letters*, **62**, pp. 300-303.
[15] Geballe, T. H. and Hull, G. W., 1955, "Seebeck Effect in Silicon," *Physical Review*, 98, 4, pp. 940-947.
[16] Yang, B., Liu, J. L., Wang, K. L. and Chen, G., 2002, "Simultaneous measurements of Seebeck coefficient and thermal conductivity across superlattice," *Applied Physics Letters*, **80**, **10**, pp. 1758-1760.
[17] Li, D., Wu, Y., Kim, P., Shi, L., Yang, P. and Majumdar, A., 2003, "Thermal Conductivity of Individual Silicon Nanowires," *Applied Physics Letters*, **83**, **14**, pp. 2934-2936.
[18] Li, D., Wu, Y., Fan, R., Yang, P. and Majumdar, A., 2003, "Thermal Conductivity of Si/SiGe Superlattice Nanowires," *Applied Physics Letters*, **83**, **15**, pp. 3186-3188.
[19] Dames, C. and Chen, G., "Theoretical phonon thermal conductivity of SiGe superlattice nanowires," 2004, *Journal of Applied Physics*, **95**, **2**, pp. 682-693.